Effects of social distancing and isolation on epidemic spreading: a dynamical density functional theory model

Michael te Vrugt,[1] Jens Bickmann,[1] and Raphael Wittkowski[1,*]

[1] *Institut für Theoretische Physik, Center for Soft Nanoscience, Westfälische Wilhelms-Universität Münster, D-48149 Münster, Germany*

For preventing the spread of epidemics such as the coronavirus disease COVID-19, social distancing and the isolation of infected persons are crucial. However, existing reaction-diffusion equations for epidemic spreading are incapable of describing these effects. We present an extended model for disease spread based on combining an SIR model with a dynamical density functional theory where social distancing and isolation of infected persons are explicitly taken into account. The model shows interesting nonequilibrium phase separation associated with a reduction of the number of infections, and allows for new insights into the control of pandemics.

Controlling the spread of infectious diseases, such as the plague [1, 2] or the Spanish flu [3], has been an important topic throughout human history [4]. Currently, it is of particular interest due to the worldwide outbreak of the coronavirus disease 2019 (COVID-19) induced by the novel coronavirus SARS-CoV-2 [5–10]. The spread of this disease is difficult to control, since the majority of infections are not detected [11]. Due to the lack of vaccines, attempts to control the pandemic have mainly focused on social distancing [12–15] and quarantine [16, 17], i.e., the general reduction of social interactions, and in particular the isolation of persons with actual or suspected infection. While political decisions on such measures require a way for predicting their effects, existing theories do not explicitly take them into account. In this article, we present a dynamical density functional theory (DDFT) [18–21] for epidemic spreading that allows to model the effect of social distancing and isolation on infection numbers.

A quantitative understanding of disease spreading can be gained from mathematical models [22–27]. A well-known theory for epidemic dynamics is the SIR model [28]

$$\dot{S} = -cSI, \tag{1}$$

$$\dot{I} = cSI - wI, \tag{2}$$

$$\dot{R} = wI, \tag{3}$$

which has already been applied to the current coronavirus outbreak [29–31]. It is a reaction-model that describes the number of susceptible S, infected I, and recovered R individuals as a function of time t. Susceptible individuals get the disease when meeting infected individuals at a rate c. Infected persons recover from the disease at a rate w. When persons have recovered, they are immune to the disease.

A drawback of this model is that it describes a spatially homogeneous dynamics, i.e., it does not take into account the fact that healthy and infected persons are not distributed homogeneously in space, even though this fact can have significant influence on the pandemic [32, 33]. To allow for spatial dynamics, disease-spreading theories such as the SIR model have been extended to reaction-diffusion equations [34–44], where a term $D_\phi\vec{\nabla}^2\phi$ with diffusion constant D_ϕ is added on the right-hand side of the dynamical equation for $\phi = S, I, R$.

Reaction-diffusion equations, however, still have the problem that they – being based on the standard diffusion equation – do not take into account particle interactions other than the reactions. This issue arises, e.g., in chemical reactions in crowded environments such as inside a cell. In this case, the reactands, which are not pointlike, cannot move freely, which prevents them from meeting and thus from reacting. To get an improved model, one can make use of the fact that the diffusion equation is a special case of DDFT. In this theory, the time evolution of a density field $\rho(\vec{r},t)$ with spatial variable $\vec{r}$ is given by

$$\partial_t\rho = \Gamma\vec{\nabla}\cdot\left(\rho\vec{\nabla}\frac{\delta F}{\delta\rho}\right) \tag{4}$$

with a mobility Γ and a free energy F. Note that we have written Eq. (4) without noise terms, which implies that $\rho(\vec{r},t)$ denotes an ensemble average [45]. The free energy is given by $F = F_{\text{id}} + F_{\text{exc}} + F_{\text{ext}}$.Its first contribution is the ideal gas free energy $F_{\text{id}} = \beta^{-1}\int \mathrm{d}^d r\,\rho(\vec{r},t)(\ln(\rho(\vec{r},t)\Lambda^d)-1)$ corresponding to a system of noninteracting particles with the inverse temperature β, number of spatial dimensions d, and thermal de Broglie wavelength Λ. If this is the only contribution, Eq. (4) reduces to the standard diffusion equation with $D = \Gamma\beta^{-1}$. The second contribution is the excess free energy F_{exc}, which takes the effect of particle interactions into account. It is typically not known exactly and has to be approximated. The third contribution F_{ext} incorporates the effect of an external potential $U_{\text{ext}}(\vec{r},t)$. DDFT can be extended to mixtures [46–49], which makes it applicable to chemical reactions. While DDFT is not an exact theory (it is based on the assumption that the density is the only slow variable in the system [50, 51]), it is nevertheless a significant improvement compared to the standard diffusion equation as it allows to incor-

porate the effects of particle interactions and generally shows excellent agreement with microscopic simulations. In particular, it allows to incorporate the effects of particle interactions such as crowding in reaction-diffusion equations. This is done by replacing the diffusion term $D\vec{\nabla}^2\phi(\vec{r},t)$ in the standard reaction-diffusion model with the right-hand side of the DDFT equation (4) [52–54]. Thus, given that its equilibrium counterpart, static density functional theory, has already been used to model crowds [55], DDFT is a very promising approach for the development of extended models for epidemic spreading. However, despite the successes of DDFT in other biological contexts such as cancer growth [56, 57], protein adsorption [58–61], ecology [62], or active matter [63–75], no attempts have been made to apply DDFT to epidemic spreading (or other types of socio-economic dynamics).

In this work, we use the idea of a reaction-diffusion DDFT to extend the SIR model given by Eqs. (1)-(3) to a (probably spatially inhomogeneous) system of *interacting* persons, which compared to existing methods allows the incorporation of social interactions and social distancing. DDFT describes the diffusive relaxation of an interacting system and is thus appropriate if we make the plausible approximation that the underlying diffusion behavior of persons is Markovian [76] and ergodic [77]. Using the Mori-Zwanzig formalism [78–82], one can connect the DDFT model and its coefficients to the dynamics of the individual persons [50, 51, 83]. The extended model reads

$$\partial_t S = \Gamma_S \vec{\nabla}\cdot\left(S\vec{\nabla}\frac{\delta F}{\delta S}\right) - cSI, \tag{5}$$

$$\partial_t I = \Gamma_I \vec{\nabla}\cdot\left(I\vec{\nabla}\frac{\delta F}{\delta I}\right) + cSI - wI - mI, \tag{6}$$

$$\partial_t R = \Gamma_R \vec{\nabla}\cdot\left(R\vec{\nabla}\frac{\delta F}{\delta R}\right) + wI. \tag{7}$$

Note that we use different mobilities Γ_S, Γ_I, and Γ_R for the different fields S, I, and R, which allows to model the fact that infected persons, who might be in quarantine, move less than healthy persons. For generality, we have added a term $-mI$ on the right-hand side of Eq. (6) to allow for death of infected persons, which occurs at a rate m (cf. SIRD model [84, 85]). Since we are mainly interested in how fast the infection spreads, we will set $m = 0$ in the following. In this case, since the total number of persons is constant, one can easily show that

$$\vec{J} = -\Gamma_S S\vec{\nabla}\frac{\delta F}{\delta S} - \Gamma_I I\vec{\nabla}\frac{\delta F}{\delta I} - \Gamma_R R\vec{\nabla}\frac{\delta F}{\delta R} \tag{8}$$

is a conserved current. The ideal gas term F_{id} in the free energy corresponds to a system of noninteracting persons and ensures that standard reaction-diffusion models for disease spreading [35] arise as a limiting case. The temperature measures the intensity of motion of the persons. A normal social life corresponds to an average temperature, while the restrictions associated with a pandemic will lead to a lower temperature. Moreover, the temperature can be position-dependent if the epidemic is dealt with differently in different places. The excess free energy F_{exc} describes interactions. This is crucial here as it allows to model effects of social distancing and self-isolation via a repulsive potential between the different persons. Social distancing is a repulsion between healthy persons, while self-isolation corresponds to a stronger repulsive potential between infected persons and other persons. Thus, we set $F_{\mathrm{exc}} = F_{\mathrm{sd}} + F_{\mathrm{si}}$ with F_{sd} describing social distancing and F_{si} self-isolation. Note that effects of such a repulsive interaction are not necessarily covered by a general reduction of the diffusivity in existing reaction-diffusion models. For example, if people practice social distancing, they will keep a certain distance (6 feet is recommended [86]) in places such as supermarkets, where persons accumulate even during a pandemic, or if people live in crowded environments, as was the case on the ship "Diamond Princess" [16]. In our model, in the cases of two particles approaching each other, which even at lower temperatures still happens, repulsive interactions will reduce the probability of a collision and thus of an infection. Existing models can only incorporate this in an effective way as a reduction of the transmission rate c, which implies, however, that properties of the disease (How infectious is it?) and measures implemented against it (Do people stay away from each other?) cannot be modelled independently. Furthermore, interactions allow for the emergence of spatio-temporal patterns. The final contribution is the external potential U_{ext}. In general, it allows to incorporate effects of confinement into DDFT. Here, it corresponds to things such as externally imposed restrictions of movement. Travel bans or the isolation of a region with high rates of infection enter the model as potential wells.

The advantage of our model compared to the standard SIR theory is that it allows – in a way that is computationally much less expensive than "microscopic" simulations, since the computational cost is independent of the number of persons [87] – to study the way in which different actions affect how the disease spreads. For example, people staying at home corresponds to reducing the temperature, quarantine measures correspond to a strongly repulsive potential between infected an healthy persons, and mass events correspond to attractive potentials.

Specifically, we assume that both types of interactions can be modelled via Gaussian pair potentials, depending on the parameters C_{sd} and C_{si} determining the strength and σ_{sd} and σ_{si} determining the range of the interactions. Combining this assumption with a Ramakrishnan-Yussouff approximation [88] for the excess free energy and a Debye-Hückel approximation [89] for the two-body correlation, we get the specific *SIR-DDFT model*

$$\begin{aligned}\partial_t S = {} & D_S\vec{\nabla}^2 S - \Gamma_S\vec{\nabla}\cdot\big(S\vec{\nabla}(C_{\mathrm{sd}}K_{\mathrm{sd}}\star(S+R) \\ & + C_{\mathrm{si}}K_{\mathrm{si}}\star I)\big) - cSI,\end{aligned} \tag{9}$$

$$\partial_t I = D_I \vec{\nabla}^2 I - \Gamma_I \vec{\nabla} \cdot \left(I \vec{\nabla} (C_{\mathrm{si}} K_{\mathrm{si}} \star (S + I + R)) \right) + cSI - wI, \tag{10}$$

$$\partial_t R = D_R \vec{\nabla}^2 R - \Gamma_R \vec{\nabla} \cdot \left(R \vec{\nabla} (C_{\mathrm{sd}} K_{\mathrm{sd}} \star (S + R) + C_{\mathrm{si}} K_{\mathrm{si}} \star I) \right) + wI \tag{11}$$

with the diffusion coefficients $D_\phi = \Gamma_\phi \beta^{-1}$ for $\phi = S, I, R$, the kernels $K_i(\vec{r}) = \exp(-\sigma_i \vec{r}^2)$ for $i = \mathrm{sd}, \mathrm{si}$, and the spatial convolution $\star$. A possible generalization is discussed in the Supplemental Material.

We begin our investigation with a linear stability analysis of this model, using a general pair potential, in order to determine whether a homogeneous state with $I = 0$, which is always a fixed point, is stable. The full calculation is given in the Supplemental Material. In the simple SIR model, the S-R plane in phase space (these are the states where everyone is healthy) becomes unstable when $cS_0 > w$, where S_0 is the initial number of susceptible persons. Thus, the pandemic cannot break out if persons recover faster than they are able to infect others. A linear stability analysis of the full model, performed under the assumption that the initial number of immune persons R_0 is small (which corresponds to a new disease) gives the eigenvalue $\lambda_1 = cS_0 - w - D_I k^2$ with the wavenumber k, such that this instability criterion still holds when interactions are present. This means that social distancing cannot stabilize a state without infected persons, and can thus not prevent the outbreak of a disease. As reported in the literature [35], the marginal stability hypothesis [90–94] gives, based on this dispersion, a front propagation speed of $v = 2\sqrt{D_I(cS_0 - w)}$. However, there are two additional eigenvalues $\lambda_{2/3} = (-D_j + j_0 \Gamma_j U_{\mathrm{sd}} \hat{h}_d(k))k^2$ with $j = S, R$ and the Fourier transformed social distancing potential $U_{\mathrm{sd}} \hat{h}_d(k)$ associated with instabilities due to interactions. Front speeds for dispersions of this form have been calculated by Archer *et al.* [92]. If both epidemic and interaction modes are unstable, the fronts might interfere, leading to interesting results depending on their different speeds.

For a further analysis, we solved Eqs. (9)-(11) numerically. We assume x and t to be dimensionless, such that all model parameters can be dimensionless too. The calculation was done in one spatial dimension on the domain $x \in [0, 1]$ with periodic boundary conditions, using an explicit finite-difference scheme with step size $\mathrm{d}x = 0.005$ (individual simulations) or $\mathrm{d}x = 0.01$ (parameter scan) and adaptive time steps. As an initial condition, we use a Gaussian peak with amplitude 1 and variance 50^{-2} centered at $x = 0.5$ for $S(x, 0)$, $I(x, 0) = 0.001 S(x, 0)$, and $R(x, 0) = 0$. Since the effect of the parameters c and w on the dynamics is known from previous studies of the SIR model, we fix their values to $c = 1$ and $w = 0.1$ to allow for an outbreak. Moreover, we set $\Gamma_S = \Gamma_I = \Gamma_R = 1$, $D_S = D_I = D_R = 0.01$, and $\sigma_{\mathrm{sd}} = \sigma_{\mathrm{si}} = 100$. The relevant control parameters are C_{sd} and C_{si}, which control the effects of social interactions that are the new aspect of our model. We assume these parameters to be ≤ 0, which corresponds to repulsive interactions.

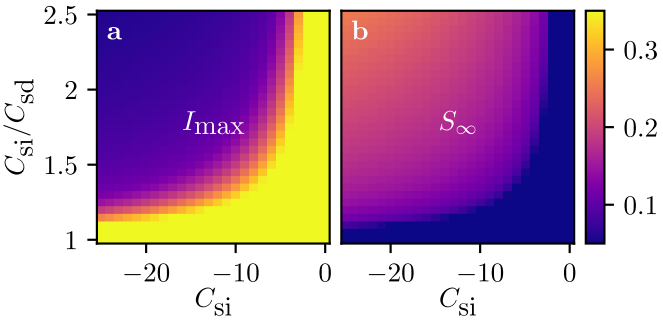

FIG. 1. Phase diagram for the SIR-DDFT model showing the dependence of (a) the maximal number of infected persons $I_{\max}$ and (b) the final number of susceptible persons S_∞ on the strength of self-isolation C_{si} and social distancing C_{sd}. A phase boundary is clearly visible.

Measures implemented against a pandemic will typically have two aims: reduction of the total number of infected persons, i.e., making sure that the final number of noninfected persons $S_\infty = \lim_{t \to \infty} S(t)$ is large, and reduction of the maximum number of infected persons $I_{\max}$ for keeping the spread within the capacities of the healthcare system. Using parameter scans, we can test whether social distancing and self-isolation can achieve those effects.

As can be seen from the phase diagrams for the SIR-DDFT model shown in Fig. 1, there is a clear phase boundary between the upper left corner, where low values of $I_{\max}$ and high values of S_∞ show that the spread of the disease has been significantly reduced, and the rest of the phase diagram, where the disease spreads in essentially the same way as in the model without social distancing. Since all simulations were performed with parameters of c and w that correspond to a disease outbreak in the usual SIR model, this shows that a reduction of social interactions can significantly inhibit epidemic spreading, and that the SIR-DDFT model is capable of demonstrating these effects. The phase boundary shows that, for a reduction of spreading by social measures, two conditions have to be satisfied. First, $|C_{\mathrm{si}}|$ has to be sufficiently large. Second, $|C_{\mathrm{si}}|$ has to be, by a certain amount, larger than $|C_{\mathrm{sd}}|$. Within our physical model of repulsively interacting particles, this arises from the fact that if healthy "particles" are repelled more strongly by other healthy particles than by infected ones, they will spend more time near infected particles and thus are more likely to be infected themselves. Physically, $|C_{\mathrm{si}}| > |C_{\mathrm{sd}}|$ is thus a very reasonable condition given that infected persons, at least once they develop symptoms, will be isolated more strongly than healthy persons. Figure 2 shows the time evolution of the total numbers $S(t)$, $I(t)$, and $R(t)$ of susceptible, infected, and recovered persons, respectively, for the cases without interactions (usual SIR model with

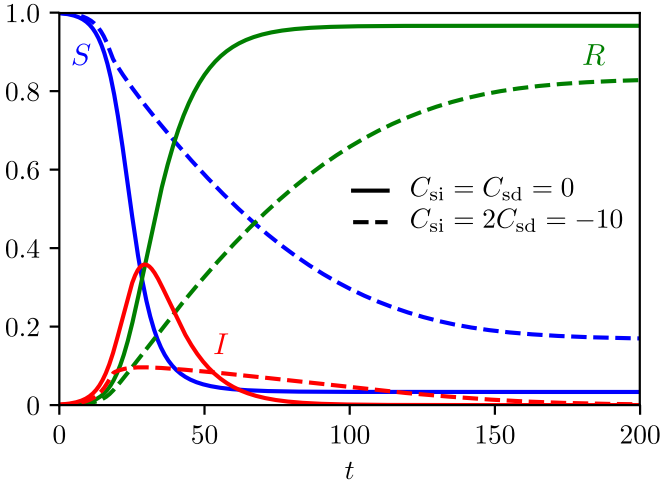

FIG. 2. Time evolution of the total number of susceptible, infected, and recovered persons for no interactions ($C_{si} = C_{sd} = 0$) and for interactions with $C_{si} = 2C_{sd} = -10$. A reduction of social contacts flattens the curve $I(t)$.

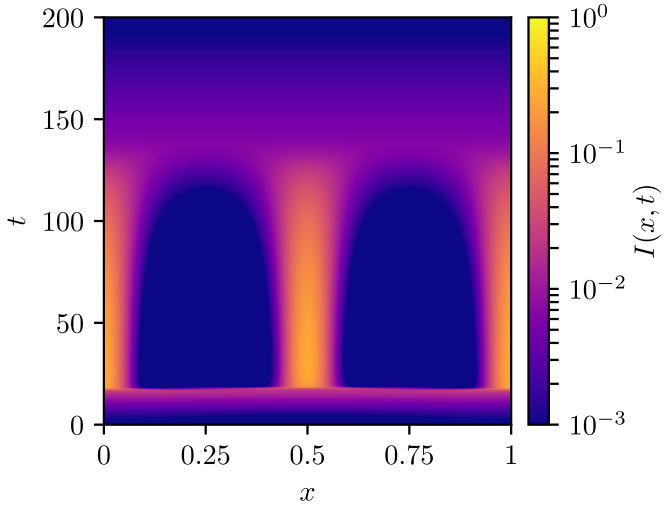

FIG. 3. Number of infected persons $I(x,t)$ as a function of space x and time t. During the epidemic spreading, the infected persons self-organize into "leper colonies".

diffusion) and with interactions (our model). If no interactions are present (i.e., $C_{si} = C_{sd} = 0$), $I(t)$ reaches a maximum value of about 0.4 and the pandemic is over at time $t \approx 100$. In the case with interactions (we choose $C_{si} = 2C_{sd} = -10$, i.e., parameter values inside the social isolation phase), the maximum is significantly reduced to a value of about 0.1. The final value of $R(t)$, which measures the total number of persons that have been infected during the pandemic, decreases from about 1.0 to about 0.8. Moreover, it takes significantly longer (until time $t \approx 200$) for the pandemic to end. This demonstrates that social distancing and self-isolation have the effects they are supposed to have, i.e., to flatten the curve $I(t)$ in such a way that the healthcare system is able to take care of all cases. The theoretical predictions for the effects of quarantine on the course of $I(t)$ (sharp rise, followed by a bend and a flat curve) are in good qualitative agreement with recent data from China [95, 96], where strict regulations were implemented to control the COVID-19 spread [17].

To explain the observed phenomena, it is helpful to analyze the spatial distribution of susceptible and infected persons during the pandemic. Figure 3 visualizes $I(x,t)$ with $x = (\vec{r})_1$. Interestingly, during the time interval where the pandemic is present, a phase separation can be observed in which the infected persons accumulate at certain spots separated from the susceptible persons. (As this effect is reminiscent of measures that used to be implemented against the spread of leprosy, we refer to these spots as "leper colonies".) This phase separation is a consequence of the interactions. Since the formation of leper colonies reduces the spatial overlap of the functions $I(x,t)$ and $S(x,t)$, i.e., the amount of contacts between infected and susceptible persons, the total number of infections decreases significantly and it takes longer until enough persons are immune to stop the pandemic.

The leper colony transition is an interesting type of nonequilibrium phase behavior in its own right. Recall that we have motivated the SIR-DDFT model based on theories for nonideal chemical reactions. It is thus very likely that effects similar to the ones observed here can be found in chemistry. In this case, they would imply that particle interactions can significantly affect the amount of a certain substance that is produced within a chemical reaction, and that such reactions are accompanied by new types of (transient) pattern formation.

In summary, we have presented a DDFT-based extension of the usual models for epidemic spreading that allows to incorporate social interactions, in particular in the form of self-isolation and social distancing. This has allowed us to analyze the effect of these measures on the spatio-temporal evolution of pandemics. Given the importance of the reduction of social interactions for the control of pandemics, the model provides a highly useful new tool for predicting epidemics and deciding how to react to them. Moreover, it shows an interesting phase behavior relevant for future work on DDFT and nonideal chemical reactions. A possible extension of our model is the incorporation of fractional derivatives [97, 98]. Furthermore, enhanced simulations in two spatial dimensions could show interesting pattern formation effects associated with leper colony formation.

ACKNOWLEDGEMENTS

R.W. is funded by the Deutsche Forschungsgemeinschaft (DFG, German Research Foundation) – WI 4170/3-1.

* Corresponding author: raphael.wittkowski@uni-muenster.de

[1] R. D. Perry and J. D. Fetherston, "Yersinia pestis-etiologic agent of plague," Clinical Microbiology Reviews **10**, 35–66 (1997).

[2] J. D. Poland and D. T. Dennis, "Plague," in *Bacterial Infections of Humans* (Springer, Boston, 1998) pp. 545–558.

[3] P. Wilton, "Spanish flu outdid WWI in number of lives claimed," Canadian Medical Association Journal **148**, 2036–2037 (1993).

[4] A. Cliff and M. Smallman-Raynor, *Oxford textbook of infectious disease control: a geographical analysis from medieval quarantine to global eradication* (Oxford University Press, Oxford, 2013).

[5] F. Wu, S. Zhao, B. Yu, Y.-M. Chen, W. Wang, Z.-G. Song, Y. Hu, Z.-W. Tao, J.-H. Tian, Y.-Y. Pei, *et al.*, "A new coronavirus associated with human respiratory disease in China," Nature **579**, 265–269 (2020).

[6] P. Zhou, X.-L. Yang, X.-G. Wang, B. Hu, L. Zhang, W. Zhang, H.-R. Si, Y. Zhu, B. Li, C.-L. Huang, *et al.*, "A pneumonia outbreak associated with a new coronavirus of probable bat origin," Nature **579**, 270–273 (2020).

[7] J. Cui, F. Li, and Z.-L. Shi, "Origin and evolution of pathogenic coronaviruses," Nature Reviews Microbiology **17**, 181–192 (2019).

[8] C. Wang, P. W. Horby, F. G. Hayden, and G. F. Gao, "A novel coronavirus outbreak of global health concern," Lancet **395**, 470–473 (2020).

[9] Q. Li, X. Guan, P. Wu, X. Wang, L. Zhou, Y. Tong, R. Ren, K. S. M. Leung, E. H. Lau, J. Y. Wong, *et al.*, "Early transmission dynamics in Wuhan, China, of novel coronavirus-infected pneumonia," New England Journal of Medicine **382**, 1199–1207 (2020).

[10] N. Zhu, D. Zhang, W. Wang, X. Li, B. Yang, J. Song, X. Zhao, B. Huang, W. Shi, R. Lu, *et al.*, "A novel coronavirus from patients with pneumonia in China, 2019," New England Journal of Medicine **382**, 727–733 (2020).

[11] R. Li, S. Pei, B. Chen, Y. Song, T. Zhang, W. Yang, and J. Shaman, "Substantial undocumented infection facilitates the rapid dissemination of novel coronavirus (SARS-CoV2)," Science, **in press**, eabb3221 (2020).

[12] R. Stein, "COVID-19 and rationally layered social distancing," International Journal of Clinical Practice, **in press**, e13501 (2020).

[13] L. Tian, X. Li, F. Qi, Q.-Y. Tang, V. Tang, J. Liu, X. Cheng, X. Li, Y. Shi, H. Liu, *et al.*, "Pre-symptomatic transmission in the evolution of the COVID-19 pandemic," preprint, **arXiv:2003.07353** (2020).

[14] A. Teslya, T. M. Pham, N. E. Godijk, M. E. Kretzschmar, M. C. Bootsma, and G. Rozhnova, "Impact of self-imposed prevention measures and short-term government intervention on mitigating and delaying a COVID-19 epidemic," preprint, **medRxiv** (2020), 10.1101/2020.03.12.20034827.

[15] N. M. Ferguson, D. Laydon, G. Nedjati-Gilani, N. Imai, K. Ainslie, M. Baguelin, S. Bhatia, A. Boonyasiri, Z. Cucunubá, G. Cuomo-Dannenburg, *et al.*, "Impact of non-pharmaceutical interventions (NPIs) to reduce COVID-19 mortality and healthcare demand," London: Imperial College COVID-19 Response Team, March 16 (2020).

[16] K. Mizumoto and G. Chowell, "Transmission potential of the novel coronavirus (COVID-19) onboard the Diamond Princess cruises ship, 2020," Infectious Disease Modelling **5**, 264–270 (2020).

[17] H. Lau, V. Khosrawipour, P. Kocbach, A. Mikolajczyk, J. Schubert, J. Bania, and T. Khosrawipour, "The positive impact of lockdown in Wuhan on containing the COVID-19 outbreak in China," Journal of Travel Medicine, **in press**, taaa037 (2020), 10.1093/jtm/taaa037.

[18] T. Munakata, "A dynamical extension of the density functional theory," Journal of the Physical Society of Japan **58**, 2434–2438 (1989).

[19] U. Marini Bettolo Marconi and P. Tarazona, "Dynamic density functional theory of fluids," Journal of Chemical Physics **110**, 8032–8044 (1999).

[20] A. J. Archer and R. Evans, "Dynamical density functional theory and its application to spinodal decomposition," Journal of Chemical Physics **121**, 4246–4254 (2004).

[21] W. Dieterich, H. L. Frisch, and A. Majhofer, "Nonlinear diffusion and density functional theory," Zeitschrift für Physik B: Condensed Matter **78**, 317–323 (1990).

[22] W. Cai, L. Chen, F. Ghanbarnejad, and P. Grassberger, "Avalanche outbreaks emerging in cooperative contagions," Nature Physics **11**, 936–940 (2015).

[23] G. E. Leventhal, A. L. Hill, M. A. Nowak, and S. Bonhoeffer, "Evolution and emergence of infectious diseases in theoretical and real-world networks," Nature Communications **6**, 6101 (2015).

[24] M. De Domenico, C. Granell, M. A. Porter, and A. Arenas, "The physics of spreading processes in multilayer networks," Nature Physics **12**, 901–906 (2016).

[25] J. Gómez-Gardenes, D. Soriano-Panos, and A. Arenas, "Critical regimes driven by recurrent mobility patterns of reaction-diffusion processes in networks," Nature Physics **14**, 391–395 (2018).

[26] F. Zarei, S. Moghimi-Araghi, and F. Ghanbarnejad, "Exact solution of generalized cooperative susceptible-infected-removed (SIR) dynamics," Physical Review E **100**, 012307 (2019).

[27] D. Soriano-Paños, F. Ghanbarnejad, S. Meloni, and J. Gómez-Gardeñes, "Markovian approach to tackle the interaction of simultaneous diseases," Physical Review E **100**, 062308 (2019).

[28] W. O. Kermack and A. G. McKendrick, "A contribution to the mathematical theory of epidemics," Proceedings of the Royal Society of London. Series A, Containing papers of a Mathematical and Physical Character **115**, 700–721 (1927).

[29] I. Nesteruk, "Statistics based predictions of coronavirus 2019-nCoV spreading in mainland China," preprint, **medRxiv** (2020), 10.1101/2020.02.12.20021931.

[30] A. Simha, R. V. Prasad, and S. Narayana, "A simple stochastic SIR model for COVID-19 infection dynamics for Karnataka: learning from Europe," preprint, **arXiv:2003.11920** (2020).

[31] A. Vivanco-Lira, "Predicting COVID-19 distribution in Mexico through a discrete and time-dependent Markov chain and an SIR-like model," preprint, **arXiv:2003.06758** (2020).

[32] P. Zhong, S. Guo, and T. Chen, "Correlation between travellers departing from Wuhan before the spring festival and subsequent spread of COVID-19 to all provinces

in China," Journal of Travel Medicine, **in press**, taaa036 (2020), 10.1093/jtm/taaa036.
[33] L. Wang and J. T. Wu, "Characterizing the dynamics underlying global spread of epidemics," Nature Communications **9**, 1–11 (2018).
[34] E. B. Postnikov and I. M. Sokolov, "Continuum description of a contact infection spread in a SIR model," Mathematical Biosciences **208**, 205–215 (2007).
[35] U. Naether, E. B. Postnikov, and I. M. Sokolov, "Infection fronts in contact disease spread," European Physical Journal B **65**, 353–359 (2008).
[36] V. Belik, T. Geisel, and D. Brockmann, "Natural human mobility patterns and spatial spread of infectious diseases," Physical Review X **1**, 011001 (2011).
[37] W. Wang, Y. Cai, M. Wu, K. Wang, and Z. Li, "Complex dynamics of a reaction-diffusion epidemic model," Nonlinear Analysis: Real World Applications **13**, 2240–2258 (2012).
[38] N. Bacaër and C. Sokhna, "A reaction-diffusion system modeling the spread of resistance to an antimalarial drug," Mathematical Biosciences & Engineering **2**, 227–238 (2005).
[39] L. J. S. Allen, B. M. Bolker, Y. Lou, and A. L. Nevai, "Asymptotic profiles of the steady states for an SIS epidemic reaction-diffusion model," Discrete and Continuous Dynamical Systems **21**, 1–20 (2008).
[40] R. Peng and S. Liu, "Global stability of the steady states of an SIS epidemic reaction-diffusion model," Nonlinear Analysis: Theory, Methods & Applications **71**, 239–247 (2009).
[41] J. Ge, K. I. Kim, Z. Lin, and H. Zhu, "A SIS reaction-diffusion-advection model in a low-risk and high-risk domain," Journal of Differential Equations **259**, 5486–5509 (2015).
[42] V. Colizza, R. Pastor-Satorras, and A. Vespignani, "Reaction-diffusion processes and metapopulation models in heterogeneous networks," Nature Physics **3**, 276–282 (2007).
[43] Y.-R. Yang, W.-T. Li, and S.-L. Wu, "Exponential stability of traveling fronts in a diffusion epidemic system with delay," Nonlinear Analysis: Real World Applications **12**, 1223–1234 (2011).
[44] S. Berres and R. Ruiz-Baier, "A fully adaptive numerical approximation for a two-dimensional epidemic model with nonlinear cross-diffusion," Nonlinear Analysis: Real World Applications **12**, 2888–2903 (2011).
[45] A. J. Archer and M. Rauscher, "Dynamical density functional theory for interacting Brownian particles: stochastic or deterministic?" Journal of Physics A: Mathematical and General **37**, 9325–9333 (2004).
[46] A. J. Archer, "Dynamical density functional theory: binary phase-separating colloidal fluid in a cavity," Journal of Physics: Condensed Matter **17**, 1405–1427 (2005).
[47] R. Roth, M. Rauscher, and A. J. Archer, "Selectivity in binary fluid mixtures: static and dynamical properties," Physical Review E **80**, 021409 (2009).
[48] R. Wittkowski, H. Löwen, and H. R. Brand, "Extended dynamical density functional theory for colloidal mixtures with temperature gradients," Journal of Chemical Physics **137**, 224904 (2012).
[49] B. Goddard, A. Nold, and S. Kalliadasis, "Multi-species dynamical density functional theory," Journal of Chemical Physics **138**, 144904 (2013).
[50] P. Español and H. Löwen, "Derivation of dynamical density functional theory using the projection operator technique," Journal of Chemical Physics **131**, 244101 (2009).
[51] M. te Vrugt and R. Wittkowski, "Projection operators in statistical mechanics: a pedagogical approach," preprint, **arXiv:2001.01572** (2019).
[52] J. F. Lutsko, "Mechanism for the stabilization of protein clusters above the solubility curve: the role of non-ideal chemical reactions," Journal of Physics: Condensed Matter **28**, 244020 (2016).
[53] J. F. Lutsko and G. Nicolis, "Mechanism for the stabilization of protein clusters above the solubility curve," Soft Matter **12**, 93–98 (2016).
[54] Y. Liu and H. Liu, "Development of reaction-diffusion DFT and its application to catalytic oxidation of NO in porous materials," AIChE Journal **66**, e16824 (2020).
[55] J. F. Méndez-Valderrama, Y. A. Kinkhabwala, J. Silver, I. Cohen, and T. A. Arias, "Density-functional fluctuation theory of crowds," Nature Chemistry **9**, 3538 (2018).
[56] A. Chauviere, H. Hatzikirou, I. G. Kevrekidis, J. S. Lowengrub, and V. Cristini, "Dynamic density functional theory of solid tumor growth: preliminary models," AIP Advances **2**, 011210 (2012).
[57] H. M. Al-Saedi, A. J. Archer, and J. Ward, "Dynamical density-functional-theory-based modeling of tissue dynamics: application to tumor growth," Physical Review E **98**, 022407 (2018).
[58] F. Fang and I. Szleifer, "Kinetics and thermodynamics of protein adsorption: a generalized molecular theoretical approach," Biophysical Journal **80**, 2568–2589 (2001).
[59] F. Fang and I. Szleifer, "Competitive adsorption in model charged protein mixtures: equilibrium isotherms and kinetics behavior," Journal of Chemical Physics **119**, 1053–1065 (2003).
[60] S. Angioletti-Uberti, M. Ballauff, and J. Dzubiella, "Dynamic density functional theory of protein adsorption on polymer-coated nanoparticles," Soft Matter **10**, 7932–7945 (2014).
[61] S. Angioletti-Uberti, M. Ballauff, and J. Dzubiella, "Competitive adsorption of multiple proteins to nanoparticles: the Vroman effect revisited," Molecular Physics **116**, 3154–3163 (2018).
[62] R. Martínez-García, J. M. Calabrese, T. Mueller, K. A. Olson, and C. López, "Optimizing the search for resources by sharing information: Mongolian gazelles as a case study," Physical Review Letters **110**, 248106 (2013).
[63] H. H. Wensink and H. Löwen, "Aggregation of self-propelled colloidal rods near confining walls," Physical Review E **78**, 031409 (2008).
[64] R. Wittkowski and H. Löwen, "Dynamical density functional theory for colloidal particles with arbitrary shape," Molecular Physics **109**, 2935–2943 (2011).
[65] A. M. Menzel, A. Saha, C. Hoell, and H. Löwen, "Dynamical density functional theory for microswimmers," Journal of Chemical Physics **144**, 024115 (2016).
[66] C. Hoell, H. Löwen, and A. M. Menzel, "Dynamical density functional theory for circle swimmers," New Journal of Physics **19**, 125004 (2017).
[67] C. Hoell, H. Löwen, and A. M. Menzel, "Particle-scale statistical theory for hydrodynamically induced polar ordering in microswimmer suspensions," Journal of Chemical Physics **149**, 144902 (2018).
[68] C. Hoell, H. Löwen, and A. M. Menzel, "Multi-species dynamical density functional theory for microswimmers:

derivation, orientational ordering, trapping potentials, and shear cells," Journal of Chemical Physics **151**, 064902 (2019).
[69] M. Enculescu and H. Stark, "Active colloidal suspensions exhibit polar order under gravity," Physical Review Letters **107**, 058301 (2011).
[70] A. Pototsky and H. Stark, "Active Brownian particles in two-dimensional traps," Europhysics Letters **98**, 50004 (2012).
[71] A. M. Menzel, T. Ohta, and H. Löwen, "Active crystals and their stability," Physical Review E **89**, 022301 (2014).
[72] R. Wittmann and J. M. Brader, "Active Brownian particles at interfaces: an effective equilibrium approach," Europhysics Letters **114**, 68004 (2016).
[73] R. Wittmann, C. Maggi, A. Sharma, A. Scacchi, J. M. Brader, and U. Marini Bettolo Marconi, "Effective equilibrium states in the colored-noise model for active matter I. Pairwise forces in the Fox and unified colored noise approximations," Journal of Statistical Mechanics: Theory and Experiment **2017**, 113207 (2017).
[74] R. Wittmann, U. Marini Bettolo Marconi, C. Maggi, and J. M. Brader, "Effective equilibrium states in the colored-noise model for active matter II. A unified framework for phase equilibria, structure and mechanical properties," Journal of Statistical Mechanics: Theory and Experiment **2017**, 113208 (2017).
[75] T. F. F. Farage, P. Krinninger, and J. M. Brader, "Effective interactions in active Brownian suspensions," Physical Review E **91**, 042310 (2015).
[76] M. te Vrugt, "The five problems of irreversibility," in preparation (2020).
[77] T. Schindler, R. Wittmann, and J. M. Brader, "Particle-conserving dynamics on the single-particle level," Physical Review E **99**, 012605 (2019).
[78] S. Nakajima, "On quantum theory of transport phenomena: steady diffusion," Progress of Theoretical Physics **20**, 948–959 (1958).
[79] H. Mori, "Transport, collective motion, and Brownian motion," Progress of Theoretical Physics **33**, 423–455 (1965).
[80] R. Zwanzig, "Ensemble method in the theory of irreversibility," Journal of Chemical Physics **33**, 1338–1341 (1960).
[81] H. Grabert, *Projection Operator Techniques in Nonequilibrium Statistical Mechanics*, 1st ed., Springer Tracts in Modern Physics, Vol. 95 (Springer-Verlag, Berlin, 1982).
[82] M. te Vrugt and R. Wittkowski, "Mori-Zwanzig projection operator formalism for far-from-equilibrium systems with time-dependent Hamiltonians," Physical Review E **99**, 062118 (2019).
[83] A. Yoshimori, "Microscopic derivation of time-dependent density functional methods," Physical Review E **71**, 031203 (2005).
[84] P. Zhu, X. Wang, S. Li, Y. Guo, and Z. Wang, "Investigation of epidemic spreading process on multiplex networks by incorporating fatal properties," Applied Mathematics and Computation **359**, 512–524 (2019).
[85] T. Berge, J. M.-S. Lubuma, G. M. Moremedi, N. Morris, and R. Kondera-Shava, "A simple mathematical model for Ebola in Africa," Journal of Biological Dynamics **11**, 42–74 (2017).
[86] W. Zhu, "Should, and how can, exercise be done during a coronavirus outbreak? An interview with Dr. Jeffrey A. Woods," Journal of Sport and Health Science **9**, 105–107 (2020).
[87] A. Malijevskỳ and A. J. Archer, "Sedimentation of a two-dimensional colloidal mixture exhibiting liquid-liquid and gas-liquid phase separation: a dynamical density functional theory study," Journal of Chemical Physics **139**, 144901 (2013).
[88] T. V. Ramakrishnan and M. Yussouff, "First-principles order-parameter theory of freezing," Physical Review B **19**, 2775–2794 (1979).
[89] J.-P. Hansen and I. R. McDonald, *Theory of Simple Liquids: with Applications to Soft Matter*, 4th ed. (Elsevier Academic Press, Oxford, 2009).
[90] G. Dee and J. S. Langer, "Propagating pattern selection," Physical Review Letters **50**, 383–386 (1983).
[91] E. Ben-Jacob, H. Brand, G. Dee, L. Kramer, and J. S. Langer, "Pattern propagation in nonlinear dissipative systems," Physica D: Nonlinear Phenomena **14**, 348–364 (1985).
[92] A. J. Archer, M. J. Robbins, U. Thiele, and E. Knobloch, "Solidification fronts in supercooled liquids: how rapid fronts can lead to disordered glassy solids," Physical Review E **86**, 031603 (2012).
[93] A. J. Archer, M. C. Walters, U. Thiele, and E. Knobloch, "Solidification in soft-core fluids: disordered solids from fast solidification fronts," Physical Review E **90**, 042404 (2014).
[94] A. J. Archer, M. C. Walters, U. Thiele, and E. Knobloch, "Generation of defects and disorder from deeply quenching a liquid to form a solid," in *Mathematical Challenges in a New Phase of Materials Science* (Springer, Kyoto, 2016) pp. 1–26.
[95] John Hopkins University, "Coronavirus COVID-19 Global Cases by the Center for Systems Science and Engineering at John Hopkins University," `https://gisanddata.maps.arcgis.com/apps/opsdashboard/index.html#/bda7594740fd40299423467b48e9ecf6`, visited 2020-03-29.
[96] H. Ellyat, W. Tan, and Y. N. Lee, "UK warns fifth of workforce could be off sick from coronavirus at its peak; army prepared," `https://www.cnbc.com/2020/03/03/coronavirus-live-updates-china-reports-125-new-cases-as-its-numbers-drop.html`, visited 2020-03-29.
[97] M. A. Khan and A. Abdon, "Dynamics of Ebola disease in the framework of different fractional derivatives," Entropy **21**, 303 (2019).
[98] S. Qureshi and A. Yusuf, "Fractional derivatives applied to MSEIR problems: comparative study with real world data," European Physical Journal Plus **134**, 171 (2019).

SUPPLEMENTAL MATERIAL

I. GENERALIZED MODEL

Here, we present a possible generalization of our model. In the main text, we have used the decomposition

$$F_{\mathrm{exc}} = F_{\mathrm{sd}} + F_{\mathrm{si}} \tag{S1}$$

with

$$F_{\mathrm{sd}} = -\int \mathrm{d}^d r \int \mathrm{d}^d r'\, C_{\mathrm{sd}} e^{-\sigma_{\mathrm{sd}}(\vec{r}-\vec{r}')^2} \left(\frac{1}{2} S(\vec{r},t) S(\vec{r}',t) + S(\vec{r},t) R(\vec{r}',t) + \frac{1}{2} R(\vec{r},t) R(\vec{r}',t) \right), \tag{S2}$$

$$F_{\mathrm{si}} = -\int \mathrm{d}^d r \int \mathrm{d}^d r'\, C_{\mathrm{si}} e^{-\sigma_{\mathrm{si}}(\vec{r}-\vec{r}')^2} I(\vec{r},t) \left(\frac{1}{2} I(\vec{r}',t) + S(\vec{r}',t) + R(\vec{r}',t) \right), \tag{S3}$$

which gives the excess free energy (i.e., the contribution from interactions) as a sum of social distancing and self-isolation. Instead, one can use the form

$$F_{\mathrm{exc}} = F_{\mathrm{sd}} + F_{\mathrm{iso}} + F_{\mathrm{ill}}. \tag{S4}$$

In this case, social distancing remains unaffected. However, there are now two terms F_{iso} and F_{ill} determining the way infected persons interact with others. F_{iso} is the isolation term, which corresponds to a repulsive interaction between infected and healthy individuals. The term F_{ill} models the interaction of infected persons with other infected persons. This can have various forms. They repel each other if they practice social distancing or self-isolation, but they can also attract each other (e.g., if they intentionally accumulate in a hospital or quarantine station). Assuming that the interaction corresponding to F_{ill} is also Gaussian, i.e.,

$$F_{\mathrm{iso}} = -\int \mathrm{d}^d r \int \mathrm{d}^d r'\, C_{\mathrm{iso}} e^{-\sigma_{\mathrm{iso}}(\vec{r}-\vec{r}')^2} I(\vec{r},t) (S(\vec{r}',t) + R(\vec{r}',t)), \tag{S5}$$

$$F_{\mathrm{ill}} = -\frac{1}{2} \int \mathrm{d}^d r \int \mathrm{d}^d r'\, C_{\mathrm{ill}} e^{-\sigma_{\mathrm{ill}}(\vec{r}-\vec{r}')^2} I(\vec{r},t) I(\vec{r}',t) \tag{S6}$$

with the parameters C_{iso} and C_{ill} for the strength and σ_{iso} and σ_{ill} for the range of the infected-noninfected and infected-infected interactions, respectively, the model given by Eqs. (9)-(11) in the main text generalizes to

$$\partial_t S = D_S \vec{\nabla}^2 S - \Gamma_S \vec{\nabla} \cdot \left(S \vec{\nabla} (C_{\mathrm{sd}} K_{\mathrm{sd}} \star (S+R) + C_{\mathrm{iso}} K_{\mathrm{iso}} \star I) \right) - cSI, \tag{S7}$$

$$\partial_t I = D_I \vec{\nabla}^2 I - \Gamma_I \vec{\nabla} \cdot \left(I \vec{\nabla} (C_{\mathrm{iso}} K_{\mathrm{iso}} \star (S+R) + C_{\mathrm{ill}} K_{\mathrm{ill}} \star I) \right) + cSI - wI, \tag{S8}$$

$$\partial_t R = D_R \vec{\nabla}^2 R - \Gamma_R \vec{\nabla} \cdot \left(R \vec{\nabla} (C_{\mathrm{sd}} K_{\mathrm{sd}} \star (S+R) + C_{\mathrm{iso}} K_{\mathrm{iso}} \star I) \right) + wI \tag{S9}$$

with the kernels

$$K_{\mathrm{iso}}(\vec{r}) = e^{-\sigma_{\mathrm{iso}} \vec{r}^2}, \tag{S10}$$

$$K_{\mathrm{ill}}(\vec{r}) = e^{-\sigma_{\mathrm{ill}} \vec{r}^2} \tag{S11}$$

and K_{sd} as defined in the main text. For $C_{\mathrm{iso}} = C_{\mathrm{ill}} = C_{\mathrm{si}}$ and $\sigma_{\mathrm{iso}} = \sigma_{\mathrm{ill}} = \sigma_{\mathrm{si}}$, the standard case is recovered. The general model can also allow for attractive interactions between infected persons, or simply for a reduction of the repulsion between them (resulting from the fact that they are already ill).

II. LINEAR STABILITY ANALYSIS

Here, we perform a linear stability analysis of the extended model given by Eqs. (5)-(7) from the main text. For the excess free energy, we use the combined Ramakrishnan-Yussouff-Debye-Hückel approximation as in Eqs. (9)-(11), but now with general two-body potentials $U_{\mathrm{sd}}h_d(x-x')$ for social distancing and $U_{\mathrm{si}}h_i(x-x')$ for self-isolation. In one spatial dimension, we obtain

$$\begin{aligned}\partial_t S(x,t) &= D_S\partial_x^2 S(x,t) - cS(x,t)I(x,t)\\ &\quad - \Gamma_S U_{\mathrm{sd}}\partial_x\bigg(S(x,t)\partial_x\int \mathrm{d}x'\, h_d(x-x')(S(x',t)+R(x',t))\bigg)\\ &\quad - \Gamma_S U_{\mathrm{si}}\partial_x\bigg(S(x,t)\partial_x\int \mathrm{d}x'\, h_i(x-x')I(x',t)\bigg),\end{aligned} \tag{S12}$$

$$\begin{aligned}\partial_t I(x,t) &= D_I\partial_x^2 I(x,t) + cS(x,t)I(x,t) - wI(x,t)\\ &\quad - \Gamma_I U_{\mathrm{si}}\partial_x\bigg(I(x,t)\partial_x\int \mathrm{d}x'\, h_i(x-x')(S(x',t)+I(x',t)+R(x',t))\bigg),\end{aligned} \tag{S13}$$

$$\begin{aligned}\partial_t R(x,t) &= D_R\partial_x^2 R(x,t) + wI(x,t)\\ &\quad - \Gamma_R U_{\mathrm{sd}}\partial_x\bigg(R(x,t)\partial_x\int \mathrm{d}x'\, h_d(x-x')(S(x',t)+R(x',t))\bigg)\\ &\quad - \Gamma_R U_{\mathrm{si}}\partial_x\bigg(R(x,t)\partial_x\int \mathrm{d}x'\, h_i(x-x')I(x',t)\bigg).\end{aligned} \tag{S14}$$

Any homogeneous state with $S=S_0$, $R=R_0$, and $I=0$, where S_0 and R_0 are constants, will be a fixed point. We consider fields $S=S_0+\tilde{S}$ and $R=R_0+\tilde{R}$ with small perturbations $\tilde{S}$ and $\tilde{R}$ and linearize in the perturbations. This results in

$$\begin{aligned}\partial_t \tilde{S}(x,t) &= D_S\partial_x^2 \tilde{S}(x,t) - cS_0 I(x,t)\\ &\quad - S_0\Gamma_S U_{\mathrm{sd}}\partial_x^2\int \mathrm{d}x'\, h_d(x-x')(\tilde{S}(x',t)+\tilde{R}(x',t))\\ &\quad - S_0\Gamma_S U_{\mathrm{si}}\partial_x^2\int \mathrm{d}x'\, h_i(x-x')I(x',t),\end{aligned} \tag{S15}$$

$$\partial_t I(x,t) = D_I\partial_x^2 I(x,t) + cS_0 I(x,t) - wI(x,t), \tag{S16}$$

$$\begin{aligned}\partial_t \tilde{R}(x,t) &= D_R\partial_x^2 \tilde{R}(x,t) + wI(x,t)\\ &\quad - R_0\Gamma_R U_{\mathrm{sd}}\partial_x^2\int \mathrm{d}x'\, h_d(x-x')(\tilde{S}(x',t)+\tilde{R}(x',t))\\ &\quad - R_0\Gamma_R U_{\mathrm{si}}\partial_x^2\int \mathrm{d}x'\, h_i(x-x')I(x',t).\end{aligned} \tag{S17}$$

We now drop the tilde and make the ansatz $S=S_1\exp(\lambda t-\mathrm{i}kx)$, $I=I_1\exp(\lambda t-\mathrm{i}kx)$, and $R=R_1\exp(\lambda t-\mathrm{i}kx)$. This gives the eigenvalue equation

$$\lambda\begin{pmatrix}S_1\\I_1\\R_1\end{pmatrix} = \begin{pmatrix}-D_Sk^2+S_0\Gamma_S U_{\mathrm{sd}}\hat{h}_d(k)k^2 & S_0\Gamma_S U_{\mathrm{si}}\hat{h}_i(k)k^2-cS_0 & S_0\Gamma_S U_{\mathrm{sd}}\hat{h}_d(k)k^2\\ 0 & -D_Ik^2+cS_0-w & 0\\ R_0\Gamma_R U_{\mathrm{sd}}\hat{h}_d(k)k^2 & w+R_0\Gamma_R U_{\mathrm{si}}\hat{h}_i(k)k^2 & -D_Rk^2+R_0\Gamma_R U_{\mathrm{sd}}\hat{h}_d(k)k^2\end{pmatrix}\begin{pmatrix}S_1\\I_1\\R_1\end{pmatrix}. \tag{S18}$$

Here, $\hat{h}_d(k)$ and $\hat{h}_i(k)$ are the Fourier transforms of $h_d(x-x')$ and $h_i(x-x')$, respectively. The corresponding characteristic polynomial reads

$$(-\lambda-D_Ik^2+cS_0-w)((-D_Sk^2+S_0\Gamma_S U_{\mathrm{sd}}\hat{h}_d(k)k^2-\lambda)(-D_Rk^2+R_0\Gamma_R U_{\mathrm{sd}}\hat{h}_d(k)k^2-\lambda)-S_0R_0k^4U_{\mathrm{sd}}^2\hat{h}_d^2(k)\Gamma_S\Gamma_R)=0. \tag{S19}$$

Rather than solving this third-order polynomial in λ exactly, we consider the limit of long wavelengths. For $k=0$, which corresponds to the usual SIR model given by Eqs. (1)-(3) in the main text if we assume $k^2\hat{h}_d(k)=0$, Eq. (S19) simplifies to

$$(-\lambda+cS_0-w)\lambda^2=0, \tag{S20}$$

which has the solutions

$$\lambda_1 = cS_0 - w, \tag{S21}$$
$$\lambda_2 = 0. \tag{S22}$$

This means that the epidemic will start growing when $cS_0 > w$, since in this case there is a positive eigenvalue. When interpreting this result, one should take into account that, since a susceptible person that has been infected cannot become susceptible again, the system will, after a small perturbation, not go back to the same state as before even if $w > cS_0$. Actually, we have tested the linear stability of the S-R plane in phase space, and the fact that any parameter combination of S_0 and R_0 with $I = 0$ is a solution of the SIR model is reflected by the existence of the eigenvalue $\lambda = 0$ with algebraic multiplicity 2 (a perturbation within the S-R plane will obviously not lead to an outbreak).

Next, we consider the case $k \neq 0$, but assume that we can neglect the term $S_0 R_0 k^4 U_{\mathrm{sd}}^2 \hat{h}_d^2(k) \Gamma_S \Gamma_R$ in Eq. (S19). This corresponds to assuming either $R_0 = 0$ (i.e., we consider the begin of an outbreak of a new disease that no one is yet immune against) or small k (such that terms of order k^4 can be neglected). Then, Eq. (S19) gives

$$(-\lambda - D_I k^2 + cS_0 - w)(-D_S k^2 + S_0 \Gamma_S U_{\mathrm{sd}} \hat{h}_d(k) k^2 - \lambda)(-D_R k^2 + R_0 \Gamma_R U_{\mathrm{sd}} \hat{h}_d(k) k^2 - \lambda) = 0. \tag{S23}$$

We can immediately read off the solutions

$$\lambda_1 = cS_0 - w - D_I k^2, \tag{S24}$$
$$\lambda_2 = -D_S k^2 + S_0 \Gamma_S U_{\mathrm{sd}} \hat{h}_d(k) k^2, \tag{S25}$$
$$\lambda_3 = -D_R k^2 + R_0 \Gamma_R U_{\mathrm{sd}} \hat{h}_d(k) k^2. \tag{S26}$$

The result for λ_1 shows that the initial state still becomes unstable for $cS_0 > w$, i.e., the interactions cannot stabilize a state without infected persons that would be unstable otherwise. The eigenvalues λ_2 and λ_3, which were 0 in the long-wavelength limit, now describe the dispersion due to interparticle interactions that may lead to instabilities not related to disease outbreak.

For determining the propagation speed of fronts, we can use the marginal stability hypothesis [90–94]. We transform to the co-moving frame that has velocity v and assume that the growth rate in this frame is zero at the leading edge. Thereby, we obtain for a general dispersion $\lambda(k)$ the equations

$$\mathrm{i}v + \frac{\mathrm{d}\lambda}{\mathrm{d}k} = 0, \tag{S27}$$
$$\mathrm{Re}(\mathrm{i}vk + \lambda) = 0. \tag{S28}$$

These equations can be solved for the complex wavenumber $k = k_{\mathrm{re}} + \mathrm{i}k_{\mathrm{im}}$ and the velocity v. For the dispersion $\lambda_1 = cS_0 - w - D_I k^2$ (we are interested in instabilities associated with infections), Eqs. (S27) and (S28) lead to

$$\mathrm{i}v - 2\mathrm{i}D_I k_{\mathrm{im}} = 0, \tag{S29}$$
$$-2D_I k_{\mathrm{re}} = 0, \tag{S30}$$
$$-vk_{\mathrm{im}} + cS_0 - w - D_I(k_{\mathrm{re}}^2 - k_{\mathrm{im}}^2) = 0. \tag{S31}$$

The solution of these equations is

$$k_{\mathrm{re}} = 0, \tag{S32}$$
$$k_{\mathrm{im}} = \pm\sqrt{\frac{cS_0 - w}{D_I}}, \tag{S33}$$
$$v = 2\sqrt{D_I(cS_0 - w)}, \tag{S34}$$

which is in agreement with results from the literature [35]. Front speeds for dispersions of the form (S25) and (S26) can be found in Ref. [92].